

Unity and Diversity of Yellow Hypergiants Family

V.G. Klochkova

Special Astrophysical Observatory RAS, Nizhnij Arkhyz, 369167 Russia

November 22, 2019

Abstract We summarize the results of long-term spectral monitoring of yellow hypergiants (YHGs) of northern hemisphere with a $R \geq 60\,000$ resolution. The spectra of these F–G stars of extremely high luminosity, compactly located at the top of the Hertzsprung–Russell diagram revealed a variety of spectral features: various types of $H\alpha$ profile, the presence (or absence) of forbidden and permitted emissions, as well as circumstellar components. Variability of spectral details of various nature is studied. Absolute luminosity, circumstellar envelope expansion rate and amplitude of pulsations are determined. The reliability of the YHG status for V1427 Aql is reliably confirmed; manifestations of a significant dynamic instability of the upper layers of the atmosphere of ρ Cas after the 2017 ejection and stratification of its gas envelope are registered; the lack of companion in the system of the V509 Cas hypergiant is proven; a conclusion is made that the V1302 Aql hypergiant is approaching to the low-temperature boundary of the Yellow Void.

Key words. stars: massive–stars: evolution–stars: atmospheres–stars: optical spectra

1. Introduction

The upper part of the Hertzsprung–Russell diagram (hereinafter, HRD), near the Humphreys–Davidson luminosity limit [1] is populated by the most massive stars in the advanced stages of evolution: luminous blue variables (LBVs), Wolf–Rayet stars, supergiants with the B[e] phenomenon, hypergiants and other unstable high-luminosity stars (hereinafter, HLSs) with emissions in the spectra. During their previous evolution, these stars were losing mass due to a quiet outflow and owing to stellar wind, the rate of which in some phases reaches critical values, entering the mode of ejection of the surface layers of matter. These stars, with an initial mass on the Main Sequence in the range of $20\text{--}60 M_{\odot}$, being at an advanced stage of evolution after the stage of red supergiants and having lost a significant fraction of their mass, have extended outflowing atmospheres and structured gas and dust envelopes, the presence of which is manifested primarily in the complex nature of spectral energy distribution (SED), as well as in the features of optical, IR and radio spectra [2]. The main groups of massive evolved stars of different masses that will be

Table 1. Selected parameters of the discussed YHG: mass loss rate $d\mathcal{M}_{\odot}/dt$, the presence of a circumstellar disk, according to [4] based on the presence of [O I] and [Ca II] emissions; the distance corresponding to parallax from [5]

Star	IR source	$\log(d\mathcal{M}_{\odot}/dt)$, $\mathcal{M}_{\odot} \text{ year}^{-1}$	Presence of disk	d , kpc
V1427 Aql	RAFGL 2343 / IRAS 19114+0002	$-2.5 \div -4.3$ [6]	+ [6]	3.22 ± 0.16
ρ Cas	RAFGL 3173 / IRAS 23518+5713	-4.85 [2]	+ [4]	1.05 ± 0.21
V509 Cas	IRC+60379 / IRAS 22579+5640	-4.92 [2]	+ [4]	4.81 ± 0.43
V1302 Aql	IRC+10420 / IRAS 19244+1115	-3.30 [2]	+ [7]	1.72 ± 0.28

considered or mentioned in the text: red supergiants (RSGs), yellow hypergiants (YHG), LBVs, blue supergiants (BSGs), hot supergiants with a B[e] phenomenon, Wolf-Rayet stars (WR). The top part of the HRD clearly presents the population density of stars of the above types in the stellar population of M 31 and M 33 galaxies [3]. The limitedness of the sample of YHG compared to the number of their immediate predecessors—RSGs is in a good light here. Probable immediate descendants of yellow hypergiants are located in the HRD areas, populated by hot supergiants of various types (BSGs, B[e]SGs, lower-luminosity LBVs).

This paper focuses on the group of dynamically unstable F–G stars of extremely high luminosity with specific spectral features. Instability manifests itself in the pulsations, stellar wind with a high mass loss rate (typical values of $d\mathcal{M}_{\odot}/dt$, see Table 1), as well as in the recurrent episodes of ejection of large masses of matter, which leads to a temporary decrease in stellar brightness and a change in its spectral class. A combination of these features allowed to distinguish these stars in a small family of yellow hypergiants. The term ‘yellow hypergiants’ was coined by de Jager [2] instead of a less convenient term *supersupergiants*. These objects are sometimes referred to as *cool hypergiants* [8]. According to the modern ideas about the evolution of massive stars, this stage is populated by stars with an initial mass in the range of about 20–40 \mathcal{M}_{\odot} [2, 9]. After the burnout of hydrogen in the core, a massive star spends most of its further existence in the stage of supergiants, whose luminosity is provided by the burning of helium in the core. Interest in these objects is due, in particular, to the fact that the observed features, which are mainly registered owing to the long-term monitoring of these rapidly evolving objects, serve as a data source for testing the models of massive star evolution and chemical composition of the Galaxy. The understanding of these final phases of evolution of massive stars is also important in the issue of supernova precursors (see the paper by Jura et al. [10]).

Currently, less than a dozen yellow hypergiants are identified in the Galaxy, all of which are listed in the survey [2]. A small number of YHG is due to the low duration of this evolutionary phase: de Jager [2] indicated the characteristic duration below 10^5 years, later Massey [11] presumed an extremely low characteristic duration, measured only in thousands of years, i.e. about 0.01% of a massive star’s lifetime. On the HRD, yellow hypergiants having the luminosity of $\log L/L_{\odot} = 5\text{--}6$ (the luminosity class of Ia⁺, according to the MK classification), occupy a limited area near the limiting luminosity [12]. In addition to extremely high luminosities, a specific property of YHG is their internal dynamic instability [13]. An instability, manifested in the pulsations and in multiple

episodes of giant masses of matter being ejected, provides for the formation of a powerful and structured circumstellar gas-and-dust envelope. Variations in the optical thickness of the envelope are revealed in a zigzag passage of the star's position on the HRD, as was observed, for example, in the star V509 Cas [12]. Quite expectable for such massive stars is a detection in the atmospheres of YHGs of large nitrogen and sodium excesses [14, 15, 16], the synthesis and dredge-up of which to the near-surface atmospheric layers occur at the previous stages of evolution of massive stars.

In this paper, we compare the observed differences in spectral and kinematic features, as well as their temporal behavior in four northern hemisphere yellow hypergiants listed in Table 1. Section 2 shortly summarizes the methods of observations and data analysis. Section 3 lists the results obtained, comparing them with those previously published, and in Section 4 we give our conclusions.

2. Spectral data

Long-term spectral monitoring of four YHGs was conducted with the NES echelle spectrograph [17, 18] placed at the Nasmyth focus of the 6-m BTA telescope of the Special Astrophysical Observatory of the Russian Academy of Sciences (SAO RAS). The NES spectrograph is equipped with a large format CCD sized 2048×2048 elements (in recent years, a 4608×2048 CCD) and is fitted with a three-slice image slicer, which reduces light loss with no spectral resolution loss. Each spectral order in the image is reiterated three times, with a shift along the dispersion of the echelle grating [18]. The spectral resolution is $\lambda/\Delta\lambda \geq 60\,000$, the signal-to-noise ratio $S/N > 100$ for all the spectra used in this work.

One-dimensional data were extracted from the 2D echelle spectra using the especially modified for the spectrograph's echelle-frame features ECHELLE context, featured in the ESO MIDAS reduction system (see the details in [19]). Traces of cosmic particles were removed by the median averaging of two echelle spectra successively obtained one after the other. Wavelength calibration was carried out using the Th–Ar hollow-cathode lamp. Further reduction including the photometric and positional measurements was performed with the latest version of the DECH20t code [20]. Note that this program code that we traditionally use to reduce the spectra allows us to measure radial velocities for separate line profile features. We only use here the heliocentric velocities V_r , the systematic errors of which, estimated from sharp interstellar components of NaI lines do not exceed 0.25 km s^{-1} (from a single line), mean random errors for shallow absorptions are of about 0.7 km s^{-1} per line.

Spectral monitoring of V1427 Aql was performed at two telescopes: the SAO RAS 6-m BTA telescope in combination with the NES spectrograph, and the McDonald Observatory 2.7-m reflector with a coude echelle spectrograph. As follows from a comparison in [16], material obtained at two telescopes is homogeneous in spectral resolution. A detailed identification of features in the spectrum of V1302 Aql was published based on the spectral atlas [21], in which the spectra of V1302 Aql and MWC 314 supergiant with the B[e] phenomenon are thoroughly compared. Identification of features in the spectra of V509 Cas, V1427 Aql and ρ Cas is conducted using the previously published spectral atlas for the F–G stars [22] and the VALD database information.

Table 2. Data on YHG based on the optical spectroscopy data: the absolute magnitude M_V , pulsation amplitude ΔV_r , envelope expansion velocity V_{exp} , microturbulent velocity ξ_t , the presence or absence of emission and its variability in the $H\alpha$ lines, forbidden emissions of [Fe II] and other metals, emissions of the doublet [Ca II] 7291 and 7324 Å, highly excited [N II] emissions

Object	V1427 Aql	ρ Cas	V509 Cas	V1302 Aql
Parameter	[16]	[26]	[27]	[28]
$W_\lambda(7773)$, Å	2.70	1.86	2.35	2.86
M_V	$-8^{\text{m}9}$	$-8^{\text{m}0}$	$-8^{\text{m}8}$	$\leq -9^{\text{m}5}$
$\log L/L_\odot$	5.47	5.11	5.43	5.71
ΔV_r , km s $^{-1}$	11	≥ 10	9	7
V_{exp} , km s $^{-1}$	≈ 11	13–23	33–40	≈ 40
ξ_t , km s $^{-1}$	6.6 4.76 ¹	12 11.1 ²	4.00 ¹ ; 11 ²	12 7.0 ²
$H\alpha$, emission	in wings var	in wings var	+ var	+ var
[Fe II], emission	–	–	+	+
[Ca II], emission	+	var ³	+	+
[N II], emission	–	–	+	–

Footnotes: 1 – data adopted from [29], 2 – from [30], 3 – [Ca II] emission is present in the spectra of ρ Cas only around the brightness minimum

3. Main parameters of yellow hypergiants

The yellow hypergiants discussed in this article are listed in Table 1, which gives the names of the associated IR sources, the most used for these stars, as well as some information needed to compare these stars. The mass loss rate for V1427 Aql is borrowed from [6], whose authors estimated the parameter by simulating the emission of CO. Further, the presence in the object of a circumstellar disk is noted according to [4], based on the presence of forbidden [Ca II] and [O I] emissions in the spectrum. The last column of this table gives distance for each star based on the parallax according to the DR2 Gaia data [5]. Extremely low distance values for V1427 Aql, ρ Cas and V1302 Aql are conspicuous here. The remoteness of these stars obtained by other methods is significantly larger: about 6 kpc for V1427 Aql according to the authors of [10], about 2.5 kpc for ρ Cas [8] and up to 5–6 kpc for V1302 Aql [7, 23]. This contradiction serves as an additional confirmation of limited parallax accuracy for stars with extended envelopes [24, 25].

Table 2 lists the parameters for YHG, obtained from spectral observations mainly on the 6-m BTA telescope. The first line of this table indicates the equivalent width $W_\lambda(7773)$ of the oxygen triplet OI 7773 Å, the well-known luminosity criterion for the evolved F–G stars. What follows is the absolute magnitude M_V corresponding to the oxygen triplet intensity using the calibration from [31]. As expected, luminosity of all four stars is very high and close to the limit. The use of the intensity of the oxygen triplet OI 7773 Å to determine the luminosity of YHG in the presence of the Gaia data is due to the specificity of stars we are investigating. Gaia’s high-precision parallaxes in Table 1 may provide exact distances, but for stars with powerful dust envelopes they do not provide the necessary

accuracy in luminosity estimates. It is useful to refer here to the study of Xu et al. [24], in which a comparison of Gaia data and VLBI radio spectroscopy data led the authors to conclude on a smaller accuracy in the Gaia data for the stars with dust envelopes. The luminosity accuracy is also limited by unreliability of the reddening estimations for stars with envelopes. A good illustration of the difficulty in the reddening estimation is presented in its detailed study for V509 Cas in [12].

3.1. Instability of yellow hypergiants

Hypergiant instability manifests itself in a weak brightness variability (with an amplitude of about 0^m2-0^m5), which is usually referred to as a pulsation type [13], as well as in the variability of the profiles of spectral features that form at different depths of the atmosphere. In the survey [2] de Jager emphasized that sometimes a star of a very high luminosity is referred to hypergiants, while a fundamental feature that distinguishes the spectrum of a supergiant of the Ia⁺ luminosity class from the spectrum of an Ia supergiant lies in large-scale motions in the atmosphere of the star, manifesting themselves in record-large absorption widths, as well as the presence of an extended envelope due to the high mass loss rate. Table 2 shows the parameters of YHGs, characterizing the dynamic instability of their atmospheres: pulsation amplitude ΔV_r , expansion velocity of the gas envelope V_{exp} , as well as the microturbulent velocity values ξ_t , obtained from the homogeneous spectral data in the studies cited in the table. To make the picture complete, we attracted the ξ_t values from [30, 29]. As follows from Table 2, microturbulent velocity is high for all hypergiants. In case of a hypergiant V1302 Aql, for which accretion of matter is detected, Table 2 lists its velocity. Note the strikingly close pulsation amplitude values, $\Delta V_r \approx 10 \text{ km s}^{-1}$, estimated from the absorptions of weak and moderate intensity, forming in the deep layers of atmosphere. It is appropriate to recall here another problem in the analysis of YHGs spectra, namely, the probable variability of microturbulent velocity at different depths in their atmospheres. This effect was first discovered by Boyarchuk et al. (see [14] and references therein) for ρ Cas. However, subsequent studies do not confirm this result [32].

Being so distinguished by the photometric and spectral properties, hypergiants belong to stars for which fixation of the evolutionary stage is difficult. Long-term studies were needed for each of them before any certainty in this task was to be achieved. For example, V1302 Aql and V1427 Aql had long been attributed to the stars in the stage after the asymptotic giant branch, inhabited by intermediate-mass stars with initial masses in the range of $2-9 M_{\odot}$ at an advanced stage of evolution with an energetically inert core and two inlayer sources of nuclear burning. After a long evolutionary path, these stars are observed in the final phase of transition to planetary nebulae and subsequently to white dwarfs, which allows them to be called protoplanetary nebulae (PPN). However, the data obtained for V1302 Aql and V1427 Aql in recent decades using different methods [1, 33, 15, 34, 35, 16, 28], allowed to come to an unambiguous interpretation of the status of these two stars as YHGs. Note that the SIMBAD database still lists for both of these stars an indication of their belonging to post-AGB stars. However, two other stars: V509 Cas and ρ Cas are catalogued as long period variables.

The reverse cases of incorrect classification of HLSs with IR excess are also known. The situation with the star V1610 Cyg, identified with the Egg nebula (= RAFGL 2688) can serve as an example to it. Owing to its high luminosity and the presence of excess infrared radiation this star was attributed to massive stars, what was noted in the survey [2]. The protoplanetary nebula phase for Egg has been confirmed by the spectral features in the radio, infrared and optical spectral ranges indicating the carbon enrichment of the stellar envelope [36, 37]. Later, reduced metallicity in the atmosphere of this star and anomalies in the abundance of chemical elements, typical for the PPN stage were detected [38].

Below, considering the individual characteristics of the spectra of YHGs, we dwell on the manifestations of the spectral variability of these objects.

3.2. Differences in the optical spectra of YHGs

Given close fundamental parameters of YHGs and in the presence of common main features in the spectra of representatives of this family (ρ Cas, V509 Cas, V1302 Aql, HD 179821), rather compactly located on the HRD, some observable properties and the features of their spectra significantly diverse, which is clearly seen at the fragments presented in Figs. 1, 2, 3 and 4. Some differences are also registered in the diversity of temporal behaviors of the features of optical spectra, which is largely due to the particularities of the structure, optical density and kinematics of the envelopes. Below we consider in more detail the features of optical spectra of four northern hemisphere YHGs, available for observations with high spectral resolution and therefore being the most studied.

In addition to the already mentioned large absorption widths, the principal feature of the optical spectra of YHGs is the presence of forbidden emissions of atoms and ions formed in the tenuous outer layers of extended atmospheres and in the circumstellar medium of these objects. The [OI] and [Ca II] emissions, also available for study from the medium-resolution spectra are studied well enough (see [39, 4] and references in these publications). These emissions are also recorded in our spectra as single-peak or two-peak features [21, 34, 28, 26, 40, 27].

3.2.1. Hypergiant V1302 Aql

The hypergiant V1302 Aql is associated with the brightest source of IR flux IRC+10420. OH-maser radiation is also registered in the system of this source [41]. Note that before this the hottest maser sources were associated only with the class M3 stars. In the framework of the classical interpretation of a two-peak OH-spectrum, an estimate of the kinematic distance to the IRC+10420 source, 6.8 kpc was made. From here followed an estimate of the absolute magnitude ($M_V < -9^m4$), well consistent with our estimate in Table 2, unusually high for an F8I supergiant. To explain the presence of maser sources in the vicinity of such a hot object a hypothesis of the formation of a powerful gas and dust envelope at the stage of an M-supergiant followed by a fast evolution of IRC+10420 to the region of higher temperatures on the HRD [42] was suggested. The assumption on the evolution of the star was confirmed later, based on the observations with high spectral resolution [43, 34, 28].

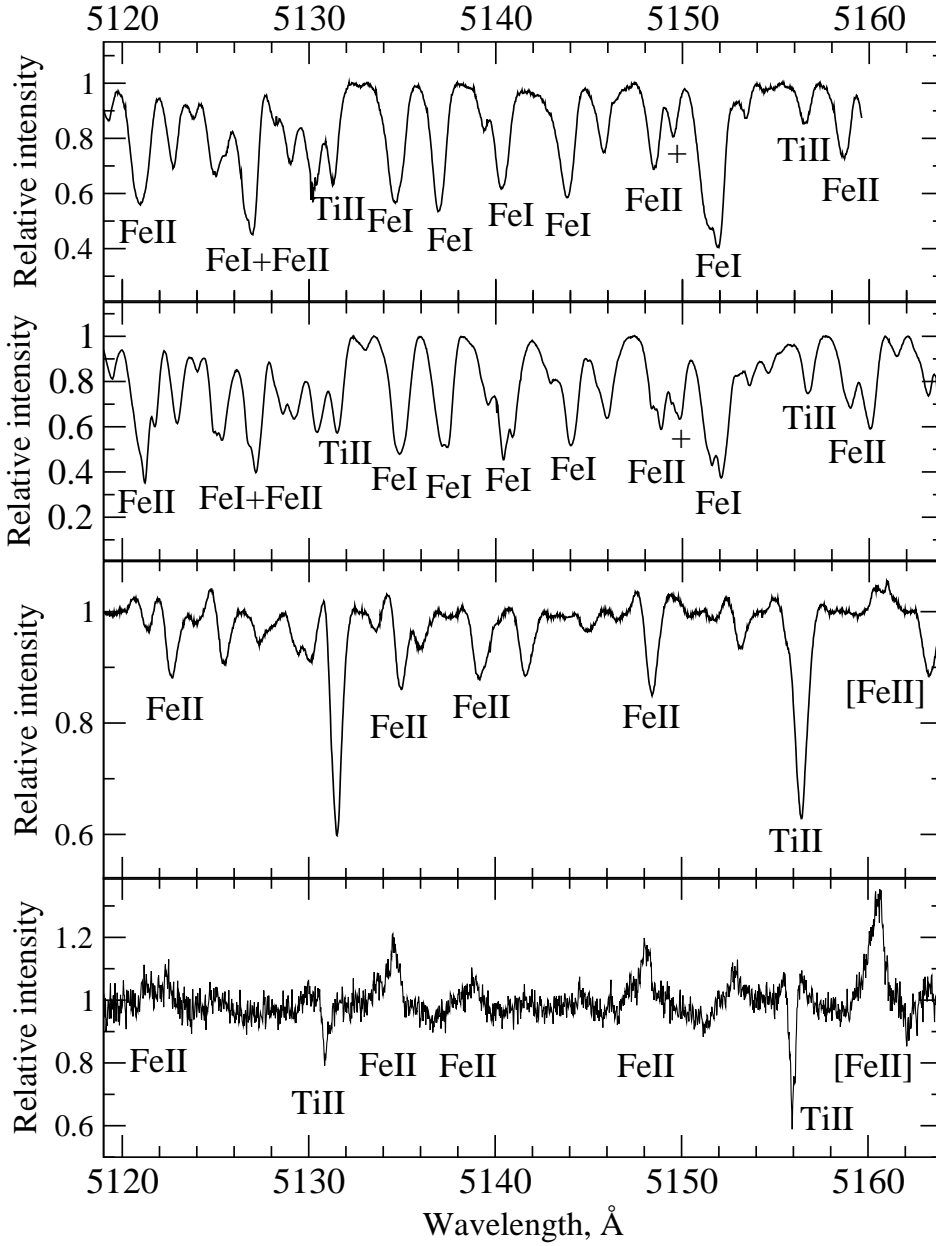


Figure 1. A comparison of the $\Delta\lambda = 5119\text{--}5164$ Å interval in the spectra of HD 179821, ρ Cas, V509 Cas and V1302 Aql (from top to bottom, in the same order as in Table 1). The main absorptions of the fragment are identified at the laboratory wavelengths. On the top two panels the cross marks the Na I 5149 Å absorption.

The optical spectrum of V1302 Aql is saturated with complex emission-absorption line profiles, forbidden emissions of [O I], [Ca II], [Fe II] and other metals of the iron group, as well as interstellar bands, DIBs. All their diversity, from pure absorptions, up to one-peak and/or two-peak forbidden and permitted emissions, are well illustrated by the spectral fragments in Figs. 1, 2, 3 and 4 and selected line profiles in Figs. 5 and 6.

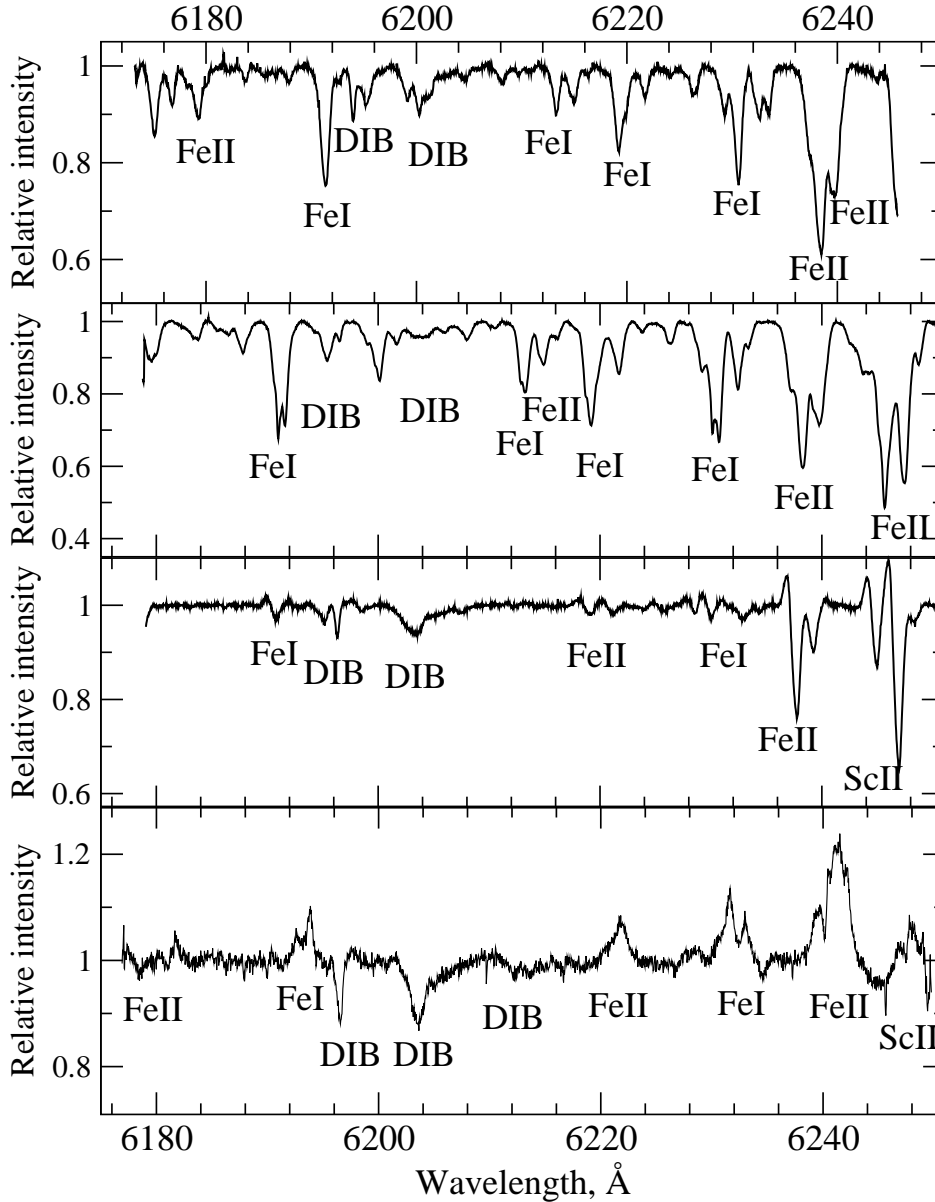


Figure 2. The same as in Fig. 1, but for the $\Delta\lambda = 6170\text{--}6250$ Å range, containing the DIBs.

Figure 7 presents $H\alpha$ profiles in two V1302 Aql spectra, obtained over different years. In the 2014 spectrum we can see the ratio of emission peak intensities, typical for the entire 20-year observation period at the 6-m telescope, where the shortwave peak is much more intense than the longwave peak [34, 45]. Only on one date of observations, November 24, 2007, we recorded an unusual shape of the $H\alpha$ profile, in which the longwave peak substantially exceeds the shortwave one [28]. A comparison of other feature profiles in the spectra of V1302 Aql for the period over 2001–2014 indicates an absence of their significant variability [28].

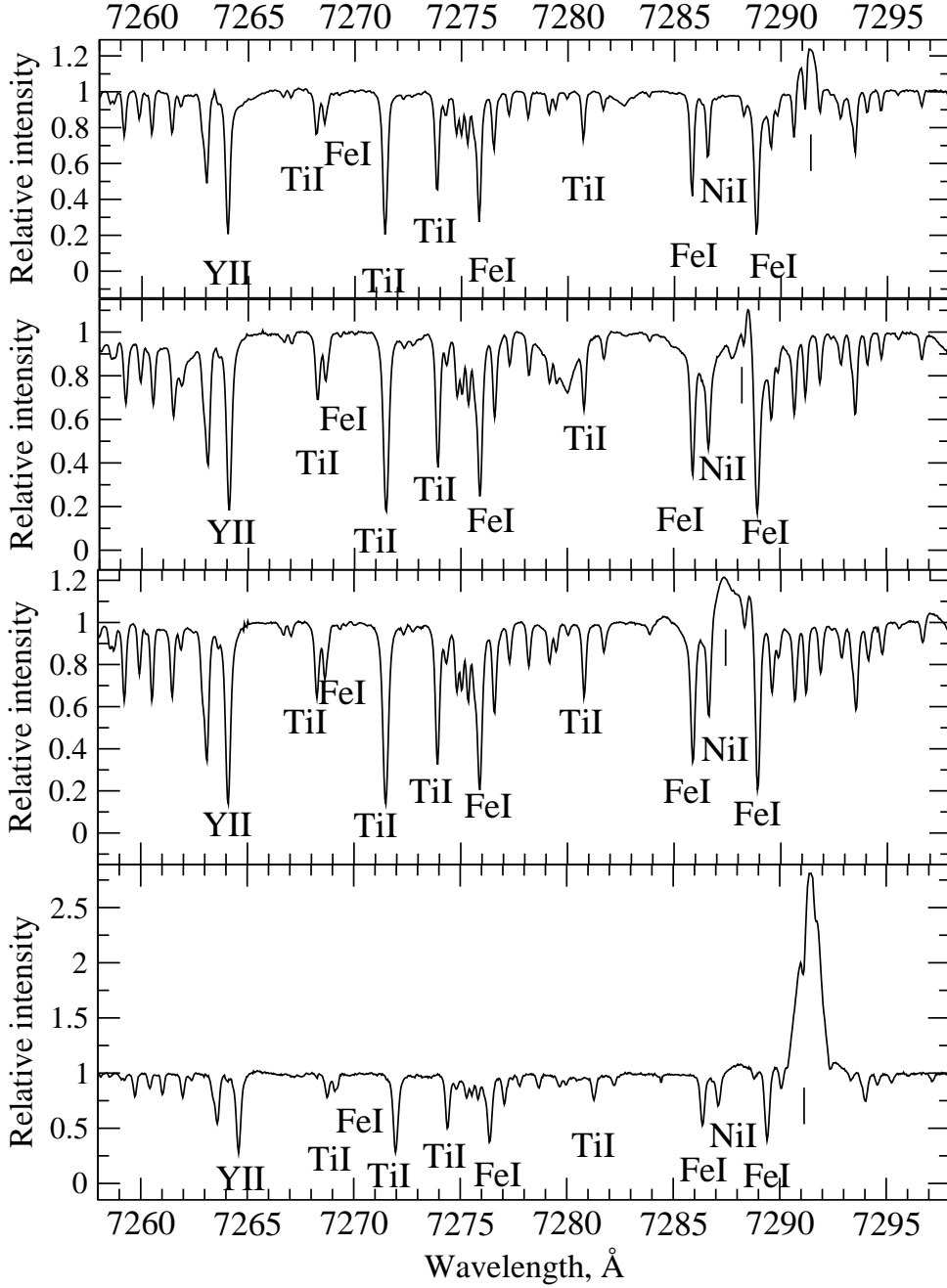


Figure 3. The same as in Fig. 1, but for the $\Delta\lambda = 7258\text{--}7298$ Å range. For ρ Cas, a fragment of the October 1, 2014 spectrum was used, i.e. after the brightness minimum. Short vertical lines mark the position of the [CaII] 7291 Å emission. The spectrum of HD 179821 is obtained with a coude echelle spectrograph of the McDonald Observatory 2.7-m reflector (see paper [16] for details).

One of decisive arguments confirming the status of a massive far-evolved HLS for V1302 Aql, was obtained based on the spectral data of the 6-m telescope, when the authors of [15] for the first time determined the chemical composition of the atmosphere of

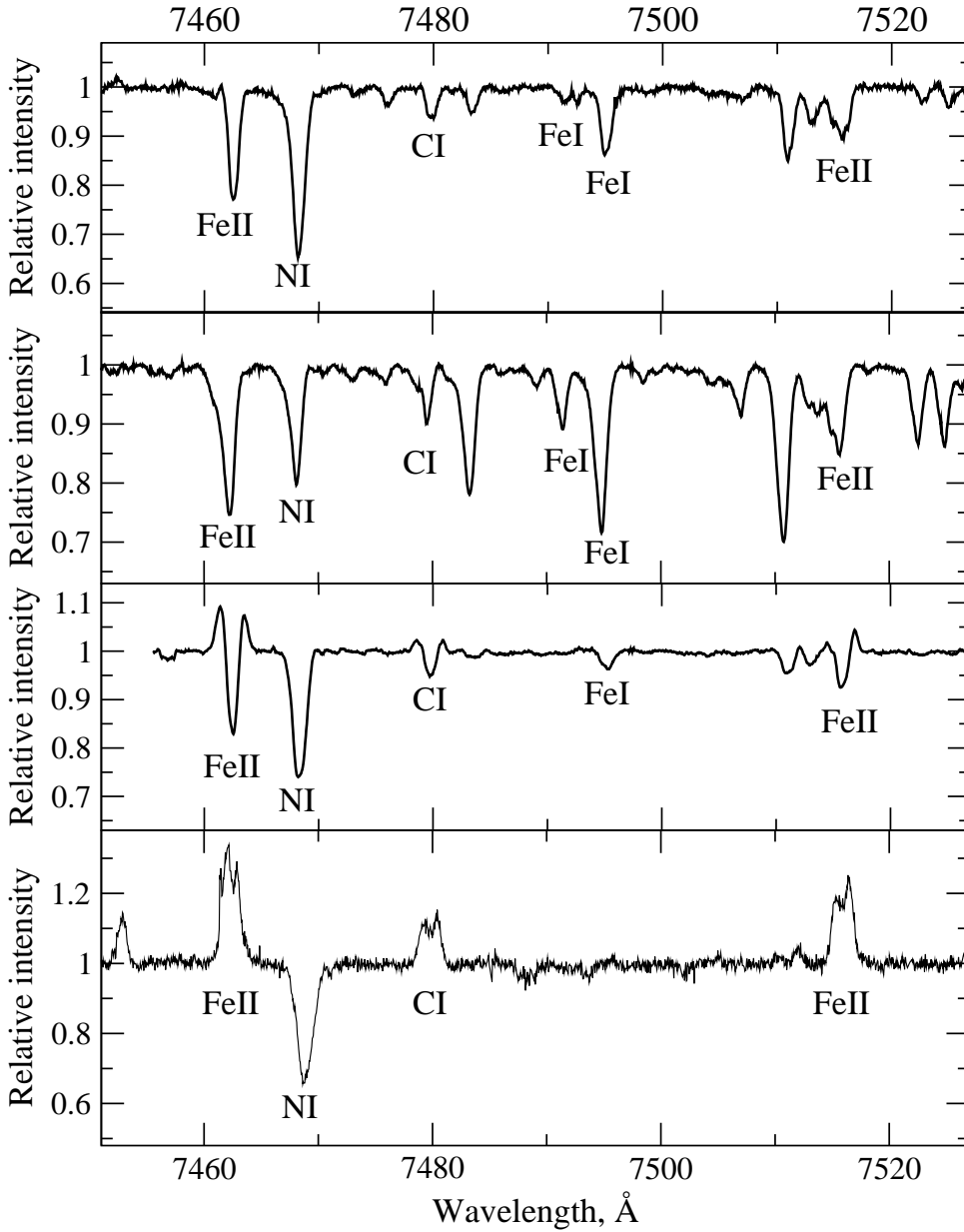


Figure 4. The same as in Fig. 3, but for the $\Delta\lambda = 7450\text{--}7530$ Å range.

V1302 Aql and found a significant excess of nitrogen. Enrichment of stellar atmosphere with nitrogen synthesized by the CNO process deep within the massive star is a distinctive sign of a large initial mass of the star. In particular, strong nitrogen absorption, along with the permitted and forbidden lines of Fe II ions, is contained in one of the 40 echelle orders of the V1302 Aql spectrum, obtained with the NES spectrograph on December 8, 2017 and shown at the bottom panel of Fig. 4. Note that later on, the authors of [46] based on the observations with the IRAM radio telescope discovered a nitrogen oxide NO molecule in the circumstellar medium of IRC+10420, which confirms the nitrogen excess in the atmosphere of its central star.

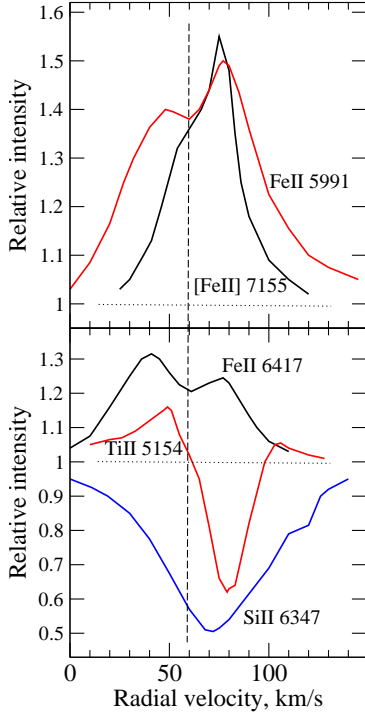


Figure 5. A variety of line profiles in the spectrum of V1302 Aql in 2014. Top panel: a forbidden [Fe II] 7155 Å emission and Fe II 5991 Å emission. Bottom panel: Fe II 6417 Å emission, emission–absorption Ti II 5154 Å line and Si II 6347 Å absorption. The dotted line describes the continuum. The vertical dashed line plots the systemic velocity $V_{\text{sys}} \approx 60 \text{ km s}^{-1}$ [44].

Interest in the hypergiant V1302 Aql intensified due to the discovery of a rapid growth of its effective temperature [44, 15, 43, 34], which allowed to assume that the star is rapidly evolving (probably, to a Wolf–Rayet stage) with a T_{eff} increase rate of about 120 K a year. The main conclusion obtained as a result of long-term spectral monitoring in [28] consists in that this YHG has entered a phase of a slowdown (or cessation) of effective temperature growth and approached the border of the Yellow Void on the HRD. It is obvious that the further monitoring of this star, observed at the evolutionary transition, whose direction is a priori difficult to predict, is indispensable. The high spectral resolution spectroscopy data are necessary to refine the structure and kinematics of its circumstellar envelope. It seems to us that the ‘rain’ model proposed by Humphries et al. [33, 45] is the most adequate with regards to the kinematic data.

3.2.2. ρ Cas, a yellow hypergiant without a dust envelope

Peculiarity of the optical spectrum of V1302 Aql is clearly manifested in comparison with a related object, a yellow hypergiant ρ Cas, whose spectrum, in contrast to the spectrum of V1302 Aql, is predominantly absorption, as illustrated in Figs. 1, 2, 3 and 4. Belonging of ρ Cas to the group of YHGs is confirmed by the features of chemical composition of its atmosphere: the content of CNO elements and a sodium excess indicate that the star

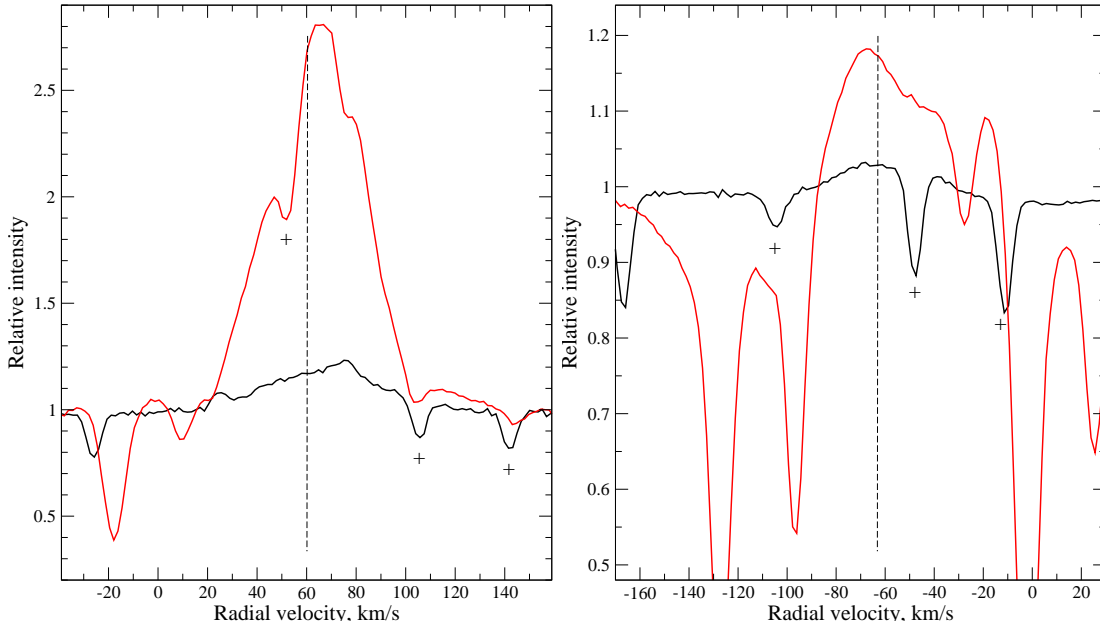


Figure 6. The profiles of forbidden emissions of [Ca II] 7291 Å (the red line) and [O I] 6300 Å in the spectra of V1302 Aql (left) and V509 Cas. Crosses indicate undeleted telluric features near the emissions. The vertical dashed line indicates the accepted value of the systemic velocity $V_{\text{sys}} \approx 60 \text{ km s}^{-1}$ for V1302 Aql [44] and $V_{\text{sys}} = -63 \text{ km s}^{-1}$ for V509 Cas [27].

has already been in the stage of red supergiants [47]. Key features of ρ Cas, which is often seen as a prototype of the YHG group, are a long-known variability of the emission-absorption H α profile [48], a high matter loss rate (it can reach up to $10^{-4} \mathcal{M}_{\odot} \text{ yr}^{-1}$, and in the 2000 episode the star for about 200 days was losing the matter at a rate of up to $3 \times 10^{-2} \mathcal{M}_{\odot} \text{ yr}^{-1}$ [49]), as well as supersonic turbulence. Besides, the optical spectrum of ρ Cas revealed a rarely observed feature—the splitting of the Ba II, Sr II, Ti II lines and other strongest absorptions with a low lower-excitation potential level (an example is presented in the bottom panel of Fig. 8). Later, these features of the ρ Cas spectrum were investigated in detail through the spectral monitoring [50, 51, 52], including spectroscopy during the 2013 and 2017 ejections [26, 40]. Spectral monitoring of ρ Cas performed at the BTA with the spectral resolution of $R \geq 60\,000$ allowed to estimate the degree of variability of effective temperature: the stellar temperature variation in the range of 5777–6744 K was found [52].

A long series of high-quality spectral observations of ρ Cas allows to study the behavior of spectral feature profiles over time, as well as the state of the velocity field in the extended atmosphere and the circumstellar environment [52, 26]. It is concluded on the closeness of velocities measured from the absorptions of iron group ions, observed in the blue part of the spectrum and the ones measured from the absorption components of lines with inverse P Cyg profiles. The position of the absorption components of lines with inverse P Cyg profiles, reflecting the presence of lumps of matter, infalling to the star with a velocity of about 20 km s^{-1} , remained stable for all the observation dates. Positions of strong Si II (multiplet 2) absorptions and absorption components of the H α and H β lines

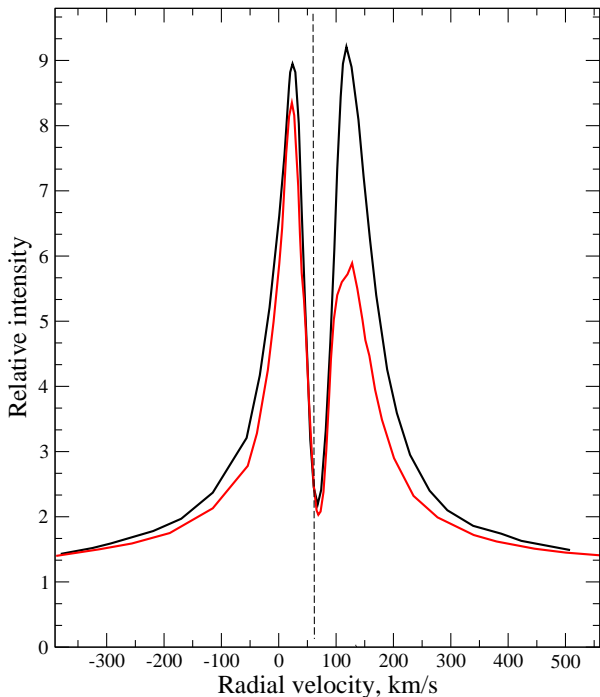


Figure 7. The $H\alpha$ profile in the spectrum of V1302 Aql in 2007 is described by the black line, and in 2014—by a red line. The vertical dashed line plots the systemic velocity $V_{\text{sys}} \approx 60 \text{ km s}^{-1}$ [44].

changed insignificantly during the observational period, staying, respectively, near the values of 63.7 and 70.5 km s^{-1} .

Owing to the broad wavelength range, the velocity field is studied from a record high number of single (several hundred in each spectrum) and split absorptions (from 12 in the visible range to 89 in the shortwave range). Radial velocity from weak symmetric metal absorptions varies from date to date with the amplitude of about $\pm 7 \text{ km s}^{-1}$ relative to the systemic velocity $V_{\text{sys}} = -47 \text{ km s}^{-1}$, which is a consequence of low-amplitude pulsations in the stellar atmosphere, a common property of YHGs. At some points, there is a dependence of radial velocity versus line intensity, indicating the existence of a velocity gradient in deep layers of the stellar atmosphere. For several phases, a difference of velocities measured from the absorptions of neutral atoms and ions was also found (at $3\text{--}4 \text{ km s}^{-1}$). Therefore, we have for the first time discovered a stratification of velocities in the atmosphere of $\rho \text{ Cas}$.

The authors of [26] showed that the long-wave component of the split absorptions of Ba II, Sr II, Ti II and other strong lines with a low lower-level excitation potential is distorted by the stationary located emission, which shifts the position of the line to the long wavelength region. Thus, the longwave components of split absorptions are common photospheric absorptions, the region of their formation and the corresponding radial velocity, taking into account a distortion by the stationary emission at certain times of observations do not differ from those in single absorptions. $\rho \text{ Cas}$ is located on the HRD at the boundary of the Yellow Void [2] dividing hypergiants and LBVs in the quiescent phase. On the boundary of the Yellow Void, the amplitude of pulsations of YHGs appar-

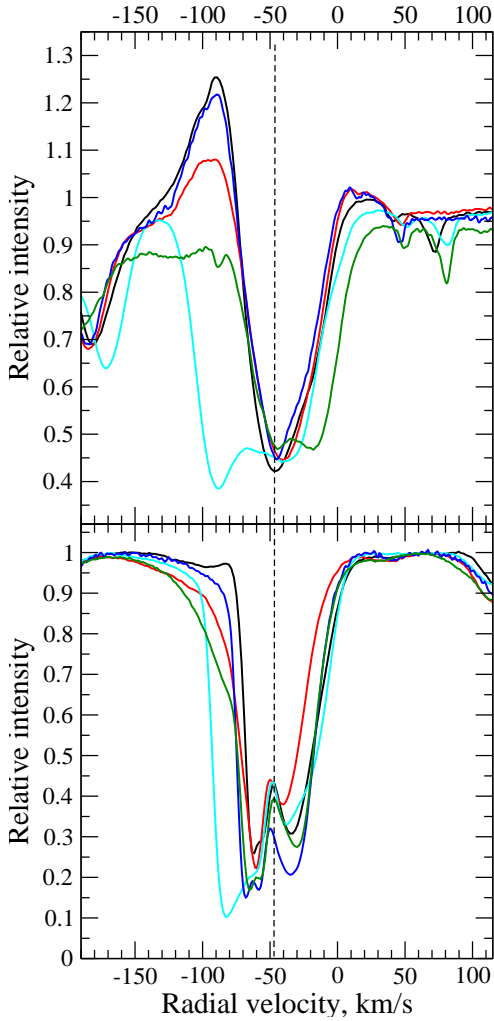


Figure 8. Variable profiles of $H\alpha$ (top panel) and $Ba\text{II}6141\text{ \AA}$ in the spectra of ρCas , obtained at the BTA during different observational sets: September 30, 2009 (in a quite state—the black solid line), February 02, 2013 (the beginning of the 2013 ejection—red), 08/07/2014 (after the 2013 minimum—cyan), February 13, 2017 (before the 2017 ejection—blue), 10/05/2017 (close to the 2017 minimum—dark green). The vertical dashed line indicates the value of $V_{\text{sys}} = -47\text{ km s}^{-1}$ [50].

ently increases rather greatly, which leads to an increased atmospheric instability and a outburst [2, 39]. In this regard, note that in the paper [26] the amplitude of the found radial velocity variability from symmetric $V_r(\text{sym})$ absorptions exceeds 10 km s^{-1} , which is higher than the $V_r(\text{sym})$ variability values in our previous study of ρCas [52].

In the summer of 2013, an ejection of matter occurred in the ρCas system, at which the star’s brightness decreased by $0^{\text{m}}5$ according to AAVSO. This ejection occurred only 12 years after the previous one in 2000–2001. Therefore, we observe an increased frequency of ejections in ρCas , which may indicate an approach of the star to crossing the border of the Yellow Void. After the 2013 ejection of matter the spectrum revealed TiO bands [40] and significant $H\alpha$ profile type variations (see more details in the article [26]). As we can see on the top panel of Fig. 8, before the flash, in the 2010 spectrum the $H\alpha$ profile had

a typical shape with an emission in the short-wavelength wing. In the 2014 spectrum, the core of the line is bifurcated for the first time. Wherein the shortwave component of the bifurcated core is offset relative to the systemic velocity by about -50 km s^{-1} , which indicates a rapid outflow of matter in the upper atmosphere after the brightness minimum.

According to the set of radial velocity measurements in the spectra of ρ Cas it is concluded that there is no correlation in the evolution of $\text{H}\alpha$ profiles and split absorptions [26]. Wherein a large velocity difference corresponding to the position of $\text{H}\alpha$ and an intermediate position of symmetric absorptions in the spectrum after the 2013 emission (see radial velocity measurement results in Fig. 5 of the article). Pulsation-type variability with an amplitude of about 10 km s^{-1} is inherent only to the symmetrical low-to-moderate-intensity absorptions, formation of which occurs in the deep atmospheric layers of the star.

A new dynamically unstable state of the gas envelope of the star is registered in 2017, which manifested itself in a substantial and quick variation of $\text{H}\alpha$ profile. In the spectrum of February 13, 2017, the $\text{H}\alpha$ profile before the 2013 outburst got restored and a short-wave emission formed again. However, a few months later, on August 6, 2017 and October 5, 2017, i.e. during an already new episode of matter ejection in October 2017, we observe significant changes: the $\text{H}\alpha$ core has split, its long-wave component has shifted into the long wavelength region by about 20 km s^{-1} relative to the systemic velocity, indicating an infall of matter.

A significant variability is also recorded in the profiles of strong split absorptions with a low lower-level excitation potential represented in particular on the bottom panel of Fig. 8. At the beginning of 2013, the $\text{Ba II } 6141 \text{ \AA}$ profile differed from the 2009 profile (i.e. before the outburst) only in the variations in the shortwave wing, where a weak emission of 2009 changed to an elongated absorption. In the 2014 spectrum (after a brightness minimum) we see a significant shift and broadening of the short-wave envelope component of the profile, indicating a velocity increase and an increase in the gradient of the matter outflow velocity. A new phenomenon in the spectrum was recorded after the 2017 outburst: in February, the splitting of profiles of strong low excitation absorptions into three components was registered for the first time, which points to a change in the structure of the upper atmosphere and the envelope of the star. We see the same picture in the October 2017 spectra near the brightness minimum.

In the long-wavelength range of the 2013 spectrum, weak envelope emissions of iron group atoms are identified, while during the 2017 episode their intensity decreased until disappearance. In the absence of emissions in the H and K nuclei of Ca II lines, envelope emissions of metals are constantly present in their wings [26].

A three-component splitting of strong absorptions allows to talk about a stratification in the uppermost layers of the outflowing atmosphere and envelope of ρ Cas, i.e. about the occurrence of two sub-envelopes with different kinematics. This new phenomenon indicates the need to continue the spectral monitoring of the star. When the signs of a new throw-off episode do appear, observations have to be carried out 1–2 times a month, which will allow to restore the temporal behavior of the kinematic state of the atmosphere and envelope and evaluate the characteristic time of variations.

3.2.3. V509 Cas, a hypergiant near the Yellow Void boundary

V509 Cas is commonly considered to be a spectroscopic twin of the hypergiant ρ Cas and therefore many authors compare their spectra [53, 54, 27]. However, a detailed study of the spectra of these two hypergiants with close fundamental parameters (mass, luminosity, stage of evolution) revealed significant differences in both the spectra and the kinematic state of the atmospheres, which indicates the difference in physical processes causing an instability of the atmospheres and envelopes. Spectral differences are manifested primarily in the difference of the $H\alpha$ profile type and its variability. $H\alpha$ profile variations in the spectrum of ρ Cas are mainly associated with the ejections. $H\alpha$ profile variations in Fig. 8 after the 2013 and 2017 ejections are particularly representative. In the spectrum of V509 Cas, the $H\alpha$ profile behaves more smoothly, as we can see in Fig. 9, the profile type, position of its long-wave components are practically unchanged. The $H\alpha$ absorption components in this figure are located on both sides of the V_{sys} line, which indicates the presence in the atmosphere and envelope of V509 Cas of both the outflowing and accreting matter. The shortwave component revealed significant variations in the intensity, shift and in its width, which is due to the variability of wind and instability of conditions in the envelope, expanding with the velocity of 33–40 km s^{-1} .

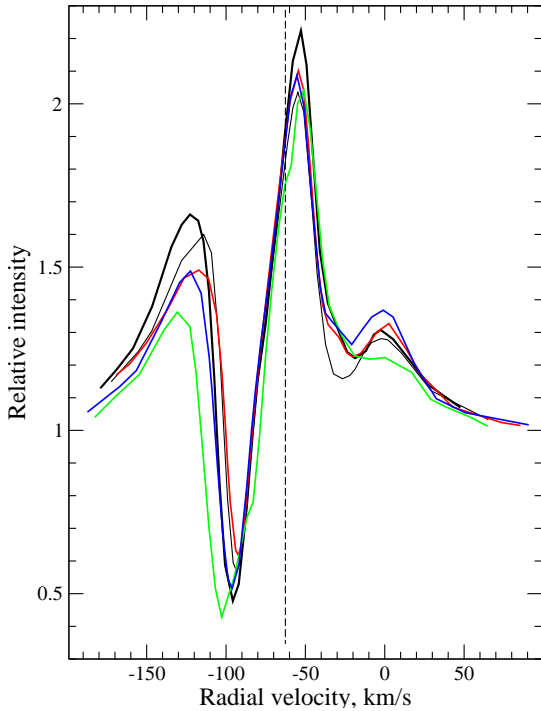


Figure 9. $H\alpha$ profile variability in the spectrum of V509 Cas: May 2, 1996—the green (dotted) line, October 1, 2014—the thick solid line, October 26, 2015—the blue line, 2017—the thin solid line, April 6, 2018—the red line. The vertical dashed line indicates the systemic velocity value $V_{\text{sys}} = -63 \text{ km s}^{-1}$, accepted in [27].

The authors of [54], comparing the spectra of V509 Cas and ρ Cas in the near UV range, also emphasized that these two stars are not spectral twins. Based on the spectral features and evolutionary status, V509 Cas is rather closer to the hypergiant V1302 Aql.

First of all, $H\alpha$ profile types are close in their spectra, which indicates a similarity of the circumstellar gas structure where these two-peak emissions are formed. However, these profiles still differ in the details, as can be seen from a comparison of Figs. 7 and 9. $H\alpha$ profile emissions in V1302 Aql are stationary located and have a small variable peak ratio [28]. Emission peaks of the $H\alpha$ profile in the spectra of V509 Cas are many times lower than in the case of V1302 Aql. Variability of the long-wave peak and the profile is in general insignificant. Short-wave emission peak intensity varies, but it is constantly below the long-wave one. No significant variations in the shape of metal line profiles and the positions of their main components are either found [27].

The optical spectrum of V509 Cas is rich in emission features, distorting the absorption profiles not only of hydrogen but also metals, which is clearly visible in the fragments of the spectrum of this star, presented in Figs. 1 and 2. Figure 6 compares the profiles of the forbidden [Ca II] 7291 and [O I] 6300 Å emissions in the spectra of V1302 Aql and V509 Cas. The profiles of [Ca II] 7291 Å emission differ significantly in their intensity, but they are single-peak in the spectra of both stars and have close half-widths: $\Delta V_r \approx 40 \text{ km s}^{-1}$. Considering the presence of forbidden [Ca II] and [O I] emissions in the spectrum (Fig. 6), we confirm a conclusion of Aret et al. [4] on the presence of a disk in the V509 Cas system. At the same time, note that our one-peak profiles in the spectra of V509 Cas obtained with high spectral resolution differ from the two-peak profiles in [4]. It is also important that the width of these emissions is about 1.5–2 times lower than this parameter in the spectrum of 3 Pup, a star with the B[e] phenomenon. Besides, as seen in Fig. 5 from [55], in the spectrum of 3 Pup the forbidden [Ca II] and [O I] emissions have two-peak profiles, which indicates the formation of these lines in the circumstellar rotating Kepler disk [56, 39].

The spectrum of V509 Cas contains a feature, rarely observed in the spectra of cool supergiants—highly excited forbidden emissions of [N II] 5755, 6548 and 6584 Å. Their presence in the spectrum of such a cool single star is hard to explain. Having forbidden [N II] lines in the spectrum of a yellow hypergiant HR 5171 has a natural explanation, the presence of a hot low-mass companion in a close binary system with a common envelope [57]. However, in case of V509 Cas the presence of such a hot companion is reliably refuted in [27].

Back in 1965, Sargent [58] emphasized that the presence of forbidden [N II] emissions and complex emission-absorption $H\alpha$ and $H \beta$ profiles indicates a probable existence of a hot envelope around V509 Cas. In the study [59] dedicated to an examination of chemical composition of the atmosphere of V509 Cas, Luck adheres to the same position. Later, Lambert and Luck [60] proposed several versions of the excitation mechanism of the forbidden [N II] line in the spectrum of V509 Cas: dissipation of mechanical energy, ionization due to UV radiation of hot stars populating an H II region in the volume of the Cep OB1 association, etc.

The authors of [61] also believe that the photons, necessary for the formation of highly excited forbidden lines, can be produced by the yellow hypergiants themselves, which demonstrate flashes on the time scale of 1–2 years with an amplitude of up to several magnitudes. An explosive flash occurring due to a release during the recombination of the hydrogen ionization energy, accumulated in the circumstellar envelope, can provide the necessary high-energy photons. A good example is a comprehensive study of the hypergiant V509 Cas parameter variations [12], which survived this kind of an episode

around 1973, during which it threw out a great amount of mass, had a large diameter and a low temperature.

Analysis of the fundamental parameters of V509 Cas over a large time interval [12] indicates that a hypergiant like V1302 Aql described a complex trajectory on the HRD. According to [60], at different stages of evolution the optical spectrum of the hypergiant varied in the spectral class range from G to K. Notwithstanding that, the luminosity class Ia was preserved. Currently, the object has approached the low-temperature boundary of the Yellow Void [12], which stimulates the further spectral monitoring of this star.

3.2.4. V1427 Aql, a cooler analogue of V1302 Aql

The complexity of YHG's research is well-illustrated by the history of study of a cool supergiant V1427 Aql = HD 179821, identified with an IR source IRAS 19114+0002. De Jager [2], reckoning V1427 Aql to the family of yellow hypergiants, called this object a 'small copy of IRC+10420'. A combination of parameters of this star for a long time did not allow to unambiguously specify its evolutionary status (see [62]). However, quite convincing evidence of V1427 Aql belonging to the YHG family has been obtained in recent years [35, 16]. Note that the results in the paper [16] are based on spectral observations with an echelle spectrometer installed at the coude focus of the McDonald Observatory 2.7-m telescope, and with the 6-m telescope in combination with the NES spectrograph. Oudmaijer et al. [35], analyzing the set of observed properties of V1427 Aql and V1302 Aql came to a conclusion that these two stars are obvious yellow hypergiants.

Comparing the parameters of yellow hypergiants given in Tables 1 and 2, we see that V1427 Aql is inferior to the members of the group only in terms of the matter outflow rate. Its main parameters, including the intensity of the OI 7773 Å triplet (and, therefore, luminosity too) and the stellar wind velocity are close to those of V1302 Aql. Modeling a map of rotational transition profiles of the ^{12}CO band, the authors of the aforementioned paper [6] obtained V_{exp} of about 35 km s^{-1} . These authors, who noted that about 10^3 years ago, the wind velocity of V1427 Aql reached an extremely high value of $3 \times 10^{-3} \mathcal{M}_{\odot} \text{ yr}^{-1}$, consider this object to be the closest relative of V1302 Aql. According to their calculations, the total mass of the envelope of V1427 Aql is four times the mass of the envelope of V1302 Aql.

Figures 1, 2, 3 and 4, illustrate the fact that the spectrum of V1427 Aql, as well as the spectrum of ρ Cas predominantly contains absorption features. An exception are the emissions in the $\text{H}\alpha$ wings, registered at individual moments, as well as a [Ca II] 7291 Å emission, which, just like in the spectra of V1302 Aql and V509 Cas, is single-peak—a narrow absorption overlapping this emission is a telluric feature at the wavelength of $\lambda = 7291.4 \text{ \AA}$.

Figure 10 illustrates $\text{H}\alpha$ profile variability in the spectrum of V1427 Aql. More data on the variability of this line is available in Fig. 2 of Sahin et al. [16]. Emission in the profile wings, if it appears, does not exceed 20% of the local continuum. The type of $\text{H}\alpha$ profile and its behavior in the spectrum of V1427 Aql is closer to that of ρ Cas. If the optical spectrum of V1427 Aql is close to the spectrum of ρ Cas, then the extended circumstellar envelope of V1427 Aql, as well as the presence of a weak [Ca II] emission, getting formed in an optically thin envelope, makes this star more akin to V1302 Aql.

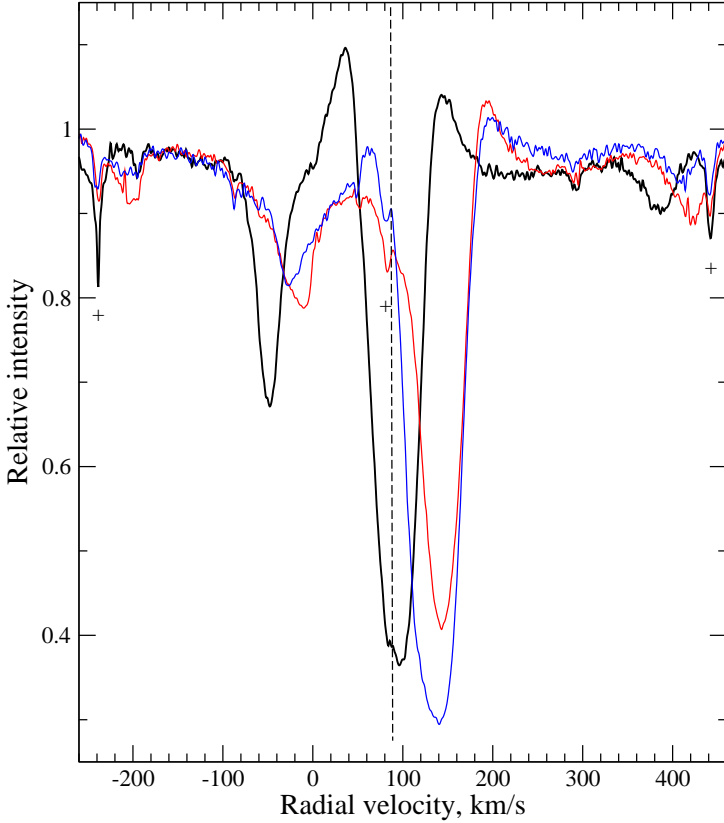


Figure 10. Variability of the H α profile in the spectrum of V1427 Aql: September 24, 2010—the blue line, May 30, 2013—the black thick line, October 9, 2013—a red line. The vertical dashed line describes the systemic velocity $V_{\text{sys}} = 86 \text{ km s}^{-1}$ [63]. Telluric features are marked by crosses.

The authors of [16] obtained critical arguments supporting the status of a massive far-evolved star for V1427 Aql. Namely, a large nitrogen and sodium excess, a high micro-turbulent velocity value and supersonic macroturbulent velocity. As it can be seen from Table 2, high luminosity of the star corresponds to a large equivalent width of the infrared oxygen triplet: $W_{\lambda}(7773) = 2.7 \text{ \AA}$. Note that such a high $W_{\lambda}(7773)$ value is measured in the spectrum of the star, for which a decreased oxygen abundance in the atmosphere was determined based on weak absorptions [16]. In general, reinforcing the conclusion of de Jager [2], we can say that V1427 Aql is a cooler and less studied analogue of the hypergiant V1302 Aql (IRC+10420), while the latter is considered a cornerstone in the study of late phases of evolution of massive stars [64].

It is obvious that our Galaxy contains also weak in the optical range, and therefore so far little studied YHGs. For example, according to the authors of [64], a distant source IRAS 18357–0604 is another twin of IRC+10420. Having high luminosity, the central star of IRAS 18357–0604 is not reachable by the means of high resolution spectroscopy due to the remoteness of the object and a large extinction in the circumstellar medium. However, according to [64], its long-wavelength spectrum, as well as the spectrum of V1302 Aql is saturated with asymmetric two-peak Paschen series H I line emissions, Ca II, low-excitation metal lines. The presence of nitrogen N I 8630 and 8729 \AA emissions in the

spectrum of IRAS 18357–0604 is an evidence of nitrogen enrichment of the atmosphere and the envelope, as in the case of IRC+10420. A particularly interesting object from the YHG family is known in the southern sky, this is a hypergiant V766 Cen = HR 5171 in a binary interacting system with a common envelope [57].

3.3. Possible relationship of YHGs and supergiants with B[e] phenomenon

The above YHGs are studied by various methods in all wavelength ranges. However, their evolutionary status is still not quite certain, since they can be attributed either to the stars, that evolve to RSG, or to stars at the stage after the RSG. Upon completion of the burning of hydrogen in the core, the descendants of RSGs make their way to the hot area of HRD. Typical representatives of RSGs are the cool red supergiants VY CMa, Betelgeuse and μ Cep with the spectral classes Sp = M2–M5 Ia. A key moment that can help solving the problem of evolutionary status is the presence or absence of a circumstellar envelope and the features of its structure, since the envelope, reflecting the history of matter loss variation parameters is a kind of a recording of the history of the star. A long-standing mystery in the YHG family is a lack of a dust envelope in ρ Cas with a matter loss rate of $\geq 10^{-4} \mathcal{M}_{\odot} \text{yr}^{-1}$ (and over $10^{-3} \mathcal{M}_{\odot} \text{yr}^{-1}$ during the ejection episodes [49]). An IR excess which is natural to expect of a star of such a high luminosity with a high matter loss rate, has for a long time not been detected in ρ Cas (see the references in [8, 65]). Wherein the presence of a circumstellar gas envelope appears in the CO molecule bands (see the papers [53, 51] and references therein), as well as in the components of the profiles of Na I, K I and low-excited lines of a number of ions [26]. The most natural factor explaining the presence (or absence) of a powerful dust envelope and its properties may be a difference in the luminosity of the star, in the matter loss rate associated with it, and ultimately, in the initial mass and the features of passage of an evolutionary phase. Apparently, as suggested by the authors of [66], we observe ρ Cas at an earlier stage of evolution than that of hypergiants with a large IR-flux excess.

In connection with the problem of fixing the evolutionary stage in individual YHGs, an urgent task is to study the evolutionary relationship between them and supergiants with B[e] phenomenon. The possibility of such a connection already follows from the relative position of these two groups of star types on the HRD. Aret et al. [39] analyzed this kind of connection between two groups of massive HLSs, based on a combination of IR flux excesses with the presence in the spectra of both groups of stars of forbidden [O I] and [Ca II] emissions, the formation of which occurs in an optically dense circumstellar disk in supergiants with a B[e] phenomenon and the subgroup of hot YHGs. Note that the [Ca II] 7291 Å emission is clearly visible in the October 1, 2014 spectrum of ρ Cas in Fig. 6. However, this feature did not exceed the continuum level in our spectra before the outburst and after 2017, when the star was in the quiescent state and its flux in the local continuum significantly exceeded the flux in the [Ca II] 7291 Å emission. We registered no emission in the [O I] 6300 Å line in the spectra of ρ Cas in any of our observational sets.

The optical spectrum of V509 Cas is similar to the spectrum of the star 3 Pup with the B[e] phenomenon. In the spectrum of this coolest representative (with the spectral class Sp = A4 Iab) of the family of supergiants with the B[e] phenomenon, a two-peaked H α with a stronger red component, forbidden [O I] 1F 6300, 6364 Å lines emissions, a

[Ca II] 1F 7291, 7324 Å doublet and emissions in some Fe II lines are registered. According to [55], in the 3 Pup spectrum only the Mg II 4481 Å line can be considered photospheric, while in the Fe II lines an envelope contribution is obvious, it gives profiles a specific shape: wings are raised by the emissions. The same feature is inherent to the profiles in the spectrum of V509 Cas too, in which the wings of even the weak lines are distorted by the emissions, which is clearly visible on the top panel of Fig. 4 at the Fe II 7462 Å line with the depth not exceeding 0.2 of the local continuum level.

Note that the authors of [57] suggested that the aforementioned hypergiant V766 Cen can evolve into a 3 Pup-type system, as it moves into the hot region of the HRD. Obviously, the hypothesis of a possible evolutionary relationship between the two groups of HLSs requires additional research, including that in the framework of the stellar-astrometric approach.

4. Conclusions

We have presented the results of a long term spectral monitoring of yellow hypergiants of the northern celestial hemisphere. Fundamental parameters of stars were determined based on the homogeneous spectroscopy data with high spectral resolution. An IR oxygen triplet OI 7773 Å with extreme equivalent width values served as a luminosity criterion: the considered stars have an average value of $\log L/L_{\odot} = 5.43 \pm 0.14$.

Based on the ensemble of detailed positional measurement data we estimated the circumstellar envelope expansion rate in the range of $11 \div 40 \text{ km s}^{-1}$. Based on the weak absorptions the amplitude of pulsations in a narrow range of values $\Delta V_r = 7 \div 11 \text{ km s}^{-1}$ was determined for four objects.

We demonstrated a diversity of observed spectral features in stars of extremely high luminosity, compactly located at the top of the Hertzsprung–Russell diagram, namely, the presence (or absence) of permitted and forbidden emissions, emission components of complex profiles, temporal features of behavior of spectral features of various nature.

High spectral resolution monitoring efficiency is shown for the detection of dynamic state variability at different depths of the extended atmosphere and circumstellar envelope of the hypergiants. In particular, due to many years of monitoring of the hypergiant V1302 Aql we conclude that it is approaching the low temperature boundary of the Yellow Void, which indicates the relevance of continuing to monitor this star.

The reliability of the hypergiant status for V1427 Aql and the lack of a companion in the V509 Cas was established. Monitoring of ρ Cas allowed to fix the dynamic instability of the upper atmosphere of the star and for the first time to detect a stratification of its gas envelope during the 2017 matter ejection episode. Due to the more frequent ejection episodes, we emphasize absolute importance of continuing the spectral monitoring of ρ Cas.

Acknowledgements. The author is grateful to his co-authors who participated in the implementation of the supergiant spectroscopy program at the BTA and in the preparation of joint publications. The author thanks The Russian Foundation for Basic Research for the financial support (project 18–02–00029 a). We made use of the astronomical databases SIMBAD, SAO/NASA ADS, AAVSO and VALD.

References

1. R. M. Humphreys and K. Davidson, *Astrophys. J.* **232**, 409 (1979).
2. C. de Jager, *Ann. Rev. Astron. Astrophys.* **8**, 145 (1998).
3. R. M. Humphreys, K. Davidson, D. Hahn, et al., *Astrophys. J.* **844**, 40 (2017).
4. A. Aret, M. Kraus, I. Kolka, and G. Maravelias, *ASP Conf. Series* **510**, 162 (2017).
5. Gaia Collaboration, A. G. A. Brown, A. Vallenari, et al., *Astron and Astrophys.* **616**, A1 (2018).
6. A. Castro-Carrizo, G. Quintana-Lacaci, V. Bujarrabal, et al., *Astron and Astrophys.* **465**, 457 (2007).
7. T. J. Jones, R. M. Humphreys, R. D. Gehrz, et al., *Astrophys. J.* **411**, 323 (1993).
8. M. T. Schuster, R. M. Humphreys, and M. Marengo, *Astron. J.* **131**, 603 (2006).
9. G. Meynet, P. Eggenberger, and A. Maeder, *IAU Symposium* **241**, 13 (2007).
10. M. Jura, T. Velusamy, and M. W. Werner, *Astrophys. J.* **556**, 408 (2001).
11. P. Massey, *New Astron. Reviews* **57**, 14 (2013).
12. H. Nieuwenhuijzen, C. De Jager, I. Kolka, et al., *Astron and Astrophys.* **546**, A105 (2012).
13. C. de Jager, A. Lobel, H. Nieuwenhuijzen, and R. Stothers, *Mon. Not. R. Astron. Soc.* **327**, 452 (2001).
14. A. A. Boyarchuk, I. Gubeny, I. Kubat, et al., *Astrophysics* **28**, 202 (1988).
15. V. G. Klochkova, E. L. Chentsov, and V. E. Panchuk, *Mon. Not. R. Astron. Soc.* **292**, 19 (1997).
16. T. Şahin, D. L. Lambert, V. G. Klochkova, and V. E. Panchuk, *Mon. Not. R. Astron. Soc.* **461**, 4071 (2016).
17. V. E. Panchuk, V. G. Klochkova, M. V. Yushkin, and I. D. Najdenov, *Journal of Optical Technology* **76**, 87 (2009).
18. V. E. Panchuk, V. G. Klochkova, and M. V. Yushkin, *Astron. Rep.* **61**, 820 (2017).
19. M. V. Yushkin and V. G. Klochkova, Preprint No. 206, (Special Astrophysical Observatory of RAS, 2004).
20. G. A. Galazutdinov, Preprint No. 92, (Special Astrophysical Observatory of RAS, 1992).
21. E. L. Chentsov, V. G. Klochkova, and N. S. Tavganskaya, *Bull Spec. Astrophys. Observatory* **48**, 25 (1999).
22. V. G. Klochkova, G. Zhao, V. E. Panchuk, and S. V. Ermakov, *Chin. J. Astron. and Astrophys.* **4**, 279 (2004).
23. J. H. Kastner and D. A. Weintraub, *Astrophys. J.* **452**, 833 (1995).

24. S. Xu, B. Zhang, M. J. Reid, et al., *Astrophys. J.* **875**, 114 (2019).
25. V. G. Klochkova and N. S. Tavalzhanskaya, *Astrophys. Bull.* **74**, 277 (2019).
26. V. G. Klochkova, V. E. Panchuk, and N. S. Tavalzhanskaya, *Astron. Rep.* **62**, 623 (2018).
95, 659 (2018).
27. V. G. Klochkova, E. L. Chentsov, and V. E. Panchuk, *Astrophys. Bull.* **74**, 41 (2019).
28. V. G. Klochkova, E. L. Chentsov, A. S. Miroshnichenko, et al., *Mon. Not. R. Astron. Soc.* **459**, 4183 (2016).
29. R. E. Luck, *Astron. J.* **147**, 137 (2014).
30. Y. Takeda and M. Takada-Hidai, *Publ. Astron. Soc. Japan* **50**, 629 (1998).
31. V. V. Kovtyukh, N. I. Gorlova, and S. I. Belik, *Mon. Not. R. Astron. Soc.* **423**, 3268 (2012).
32. A. Lobel, L. Achmad, C. de Jager, and H. Nieuwenhuijzen, *Astron and Astrophys.* **256**, 159 (1992).
33. R. M. Humphreys, N. Smith, K. Davidson, et al., *Astron. J.* **114**, 2778 (1997).
34. V. G. Klochkova, M. V. Yushkin, E. L. Chentsov, and V. E. Panchuk, *Astron. Rep.* **46**, 139 (2002). **79**, 158 (2002).
35. R. D. Oudmaijer, B. Davies, W. J. de Wit, and M. Patel, *ASP Conf. Series* **412**, 17 (2009).
36. E. J. Bakker, E. F. van Dishoeck, L. B. F. M. Waters, and T. Schoenmaker, *Astron and Astrophys.* **323**, 469 (1997).
37. C. Loup, T. Forveille, A. Omont, and J. F. Paul, *Astron and Astrophys. Suppl.* **99**, 291 (1993).
38. V. G. Klochkova, R. Szczerba, and V. E. Panchuk, *Astron. Let.* **26**, 439 (2000).
39. A. Aret, M. Kraus, I. Kolka, and G. Maravelias, *ASP Conf. Series* **508**, 357 (2017).
40. M. Kraus, I. Kolka, A. Aret, et al., *Mon. Not. R. Astron. Soc.* **483**, 3792 (2019).
41. P. T. Giguere, N. J. Woolf, and J. C. Webber, *Astrophys. J.* **207**, L195 (1976).
42. R. L. Mutel, J. M. Benson, J. D. Fix, and J. C. Webber, *Astrophys. J.* **228**, 771 (1979).
43. R. D. Oudmaijer, *Astron and Astrophys. Suppl.* **129**, 541 (1998).
44. R. D. Oudmaijer, M. A. T. Groenewegen, H. E. Matthews, et al., *Mon. Not. R. Astron. Soc.* **280**, 1062 (1996).
45. R. M. Humphreys, K. Davidson, and N. Smith, *Astron. J.* **124**, 1026 (2002).
46. G. Quintana-Lacaci, M. Agúndez, J. Cernicharo, et al., *Astron and Astrophys.* **560**, L2 (2013).
47. Y. Takeda and M. Takada-Hidai, *Publ. Astron. Soc. Japan* **46**, 395 (1994).

48. W. L. W. Sargent, *Astrophys. J.* **134**, 142 (1961).
49. A. Lobel, A. K. Dupree, R. P. Stefanik, et al., *Astrophys. J.* **583**, 923 (2003).
50. A. Lobel, G. Israelian, C. de Jager, et al., *Astron and Astrophys.* **330**, 659 (1998).
51. N. Gorlova, A. Lobel, A. J. Burgasser, et al., *Astrophys. J.* **651**, 1130 (2006).
52. V. G. Klochkova, V. E. Panchuk, N. S. Tavalzhanskaya, and I. A. Usenko, *Astron. Rep.* **58**, 101 (2014).
53. D. L. Lambert, K. H. Hinkle, and D. N. B. Hall, *Astrophys. J.* **248**, 638 (1981).
54. G. Israelian, A. Lobel, and M. R. Schmidt, *Astrophys. J.* **523**, L145 (1999).
55. E. L. Chentsov, V. G. Klochkova, and A. S. Miroshnichenko, *Astrophys. Bull.* **65**, 150 (2010). 159 (2010).
56. A. Aret, M. Kraus, and M. Šlechta, *Mon. Not. R. Astron. Soc.* **456**, 1424 (2016).
57. O. Chesneau, A. Meilland, E. Chapellier, et al., *Astron and Astrophys.* **563**, A71 (2014).
58. W. L. W. Sargent, *The Observatory* **85**, 33 (1965).
59. R. E. Luck, *Astrophys. J.* **202**, 743 (1975).
60. D. L. Lambert and R. E. Luck, *Mon. Not. R. Astron. Soc.* **184**, 405 (1978).
61. A. M. van Genderen, H. Nieuwenhuijzen, and A. Lobel, *Astron and Astrophys.* **583**, A98 (2015).
62. B. E. Reddy and B. J. Hrivnak, *Astron. J.* **117**, 1834 (1999).
63. L. Likkell, A. Omont, M. Morris, and T. Forveille, *Astron and Astrophys.* **173**, L11 (1987).
64. J. S. Clark, I. Negueruela, and C. González-Fernández, *Astron and Astrophys.* **561**, A15 (2014).
65. D. Shenoy, R. M. Humphreys, T. J. Jones, et al., *Astron. J.* **151**, 51 (2016).
66. G. Quintana-Lacaci, V. Bujarrabal, and A. Castro-Carrizo, *Astron and Astrophys.* **488**, 203 (2008).